Supporting Information
Catalytic Oxidation of Propane over Palladium Alloyed with Gold: An Assessment of the Chemical and Intermediate Species

Haval Kareem,[a] Shiyao Shan,[a] Zhi-Peng Wu,[a] Leslie Velasco,[a] Kelli Moseman,[a] Casey P. O'Brien,[c] Ivan c. Lee,[c*] Dat T.Tran,[c] Yazan Maswadeh,[b] Lefu Yang,[d] Derrick Mott,[e] Jin Luo,[a] Valeri Petkov,[b*] and Chuan-Jian Zhong [a,*]

[a)] Department of Chemistry, State University of New York at Binghamton, Binghamton, NY 13902, USA
[b)] Department of Physics, Central Michigan University, Mt. Pleasant, Michigan 48859, USA
[c)] U.S. Army Research Laboratory, Sensors and Electron Devices Directorate, Adelphi, MD 20783, USA
[d)] College of Chemistry and Chemical Engineering, Xiamen University, Xiamen 361005, China
[e)] School of Materials Science, Japan Advanced Institute of Science and Technology, Nomi, Ishikawa 923-1292, Japan

Additional HAADF-STEM image, characterization, and catalytic activity data:

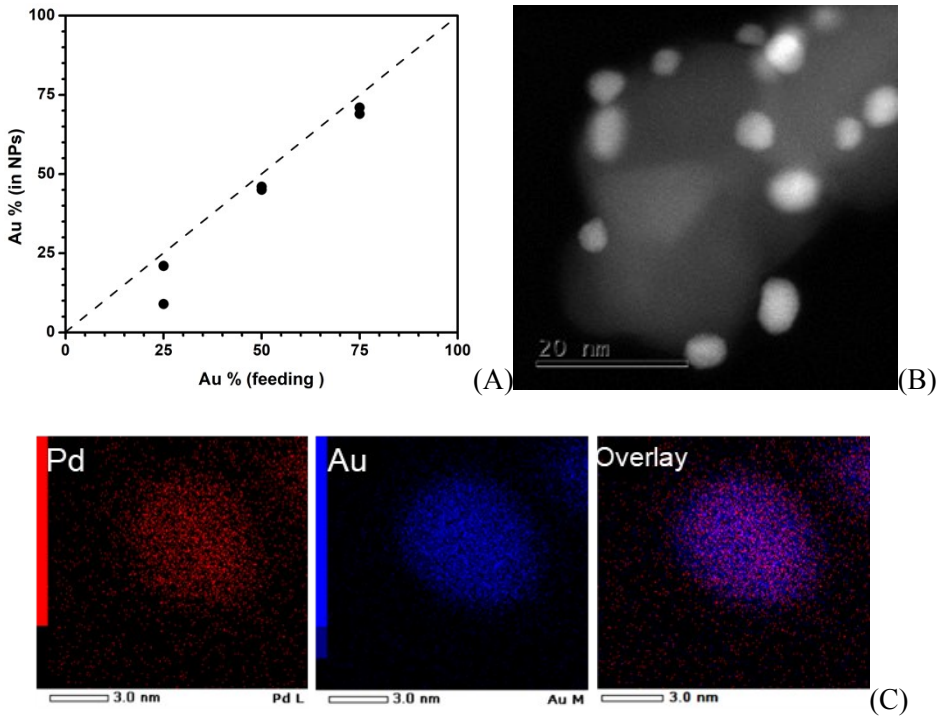

Fig. S1. (A) Plot of Au composition in the as-synthesized PdAu nanoparticles (determined by ICP) vs. Au-precursor composition in the synthetic feeding composition. The dashed line represents a 1:1 relationship. The solid line represents the linear fitting to the NPs data (slope: 1.2, R2 = 0.974. (B) HAADF-STEM images for $Pd_{55}Au_{45}/TiO_2$ nanoparticles. (C) EDS mapping of Pd and Au in a representative sample of $Pd_{55}Au_4/TiO_2$.

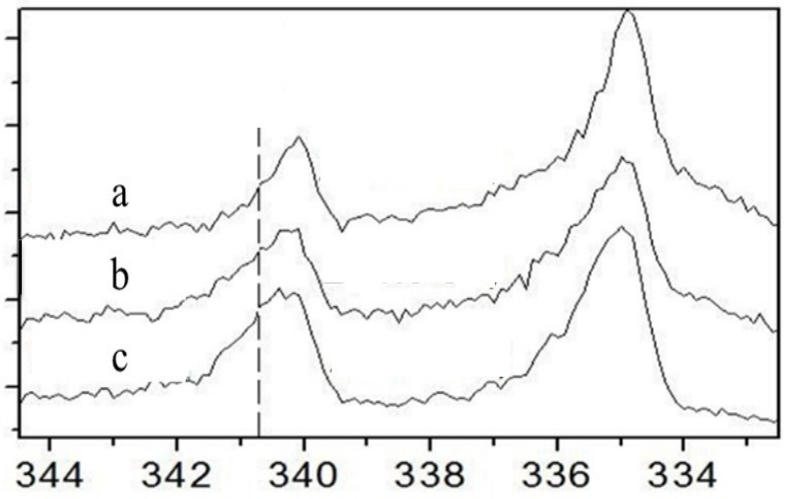

Fig.**S2**. XPS spectra in the Pd(3d) region for $Pd_{31}Au_{69}$ (a), $Pd_{55}Au_{45}$ (b), and $Pd_{91}Au_{9}$ (c). The dashed line is for comparison of the relative shifts of the peak positions of Pd $3d_{3/2}$ and $3d_{5/2}$ (~340.2 eV and ~335 eV). There is a downshift for Pd $3d_{3/2}$ (0.5 eV (a), 0.3 eV (b), and 0.4 eV (c)). This peak position is largely characteristic of Pd(0) state, which is supported by the fact that no oxygen species (at 343 eV) were detected[26]. The subtle shifts are a result of charge transfer from Au to Pd (*d*-electron) in the AuPd alloys.

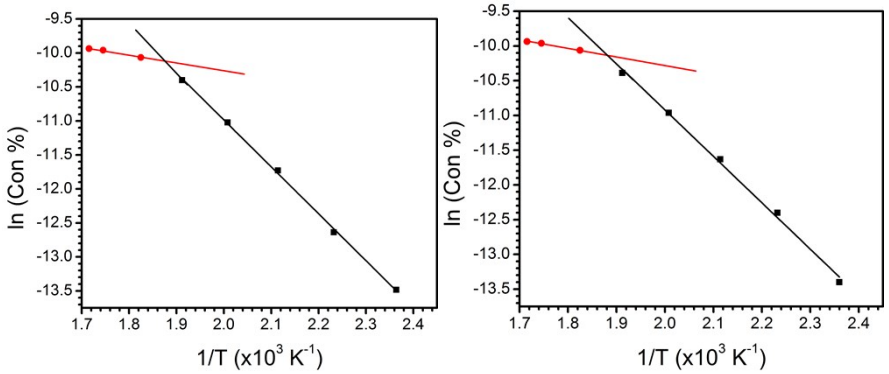

(A) (B)

Fig.S3 Arrhenius plot For $Pd_{55}Au_{45}/TiO_2$ for propane oxidation as fresh state (A), and O_2 treated (B), low temperature (black) and high temperature (red)

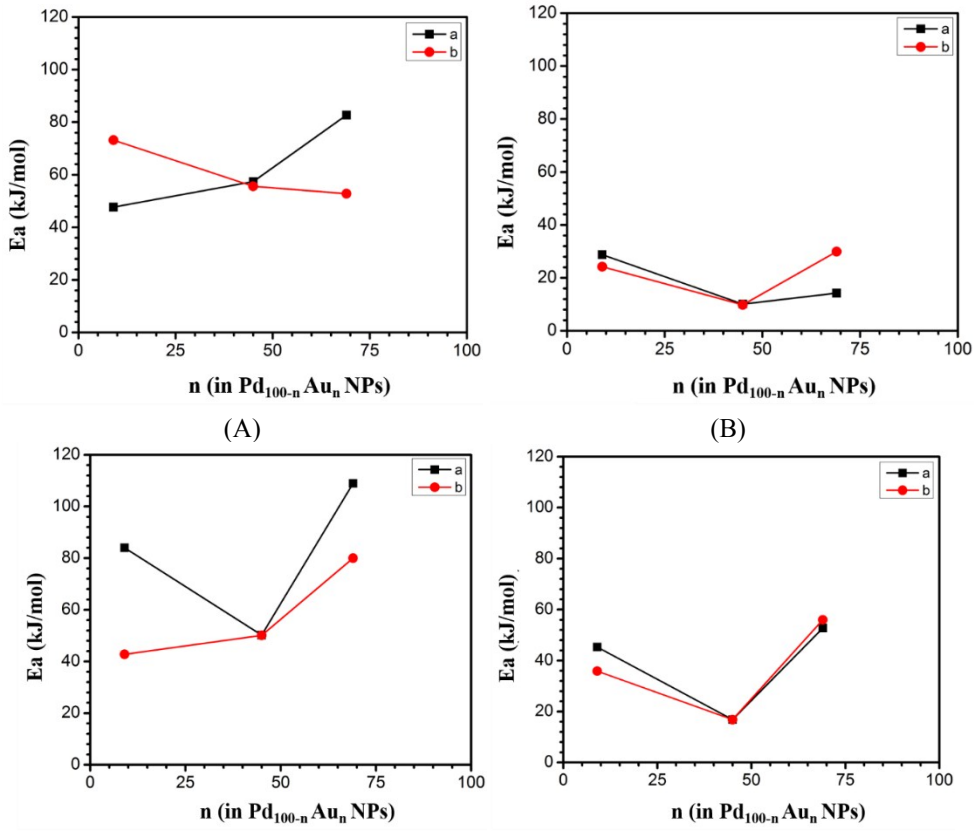

Fig. S4 Activation energy (E_a) vs. Au% (n) in the low temperature (A-C) and the high temperature (B-D) ranges for propane oxidation over $Pd_{100-n}Au_n/TiO_2$ (A-B) and over $Pd_{100-n}Au_n/Al_2O_3$ (C-D) catalysts: freshly-prepared (a), and after O_2 treatment (b).

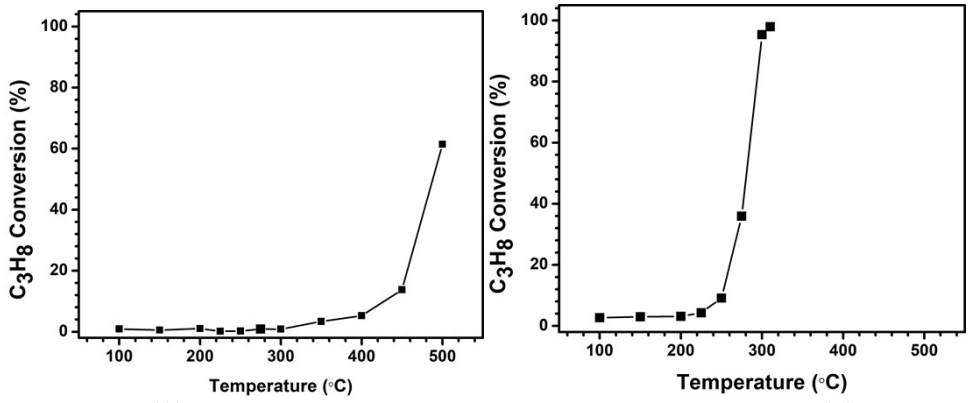

Fig. S5. Plots of propane oxidation activities over Au/TiO_2 (A) , and Pd/Al_2O_3 (B).

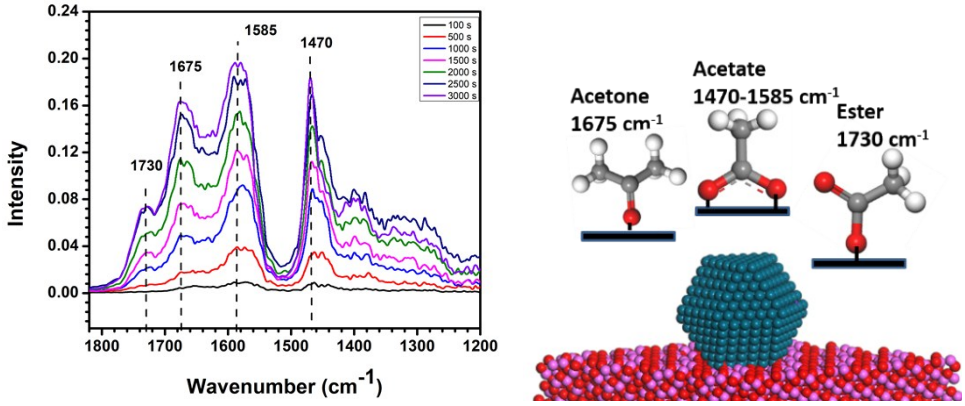

(A) (B)

Figure S6. (A) In-situ DRIFTS spectra recorded during propane oxidation over Pd/Al_2O_3 (commercial) at 275 °C; The spectra in the right are zoomed views of the spectra in the 1730 to1330 cm^{-1} region; and (B) Illustrations of **i**n-situ DRIFTs study of intermediate species detection of propane oxidation over Pd/Al2O3. Pd (green), Au (yellow), C (gray), H (white), O (red),), and Al (pink).

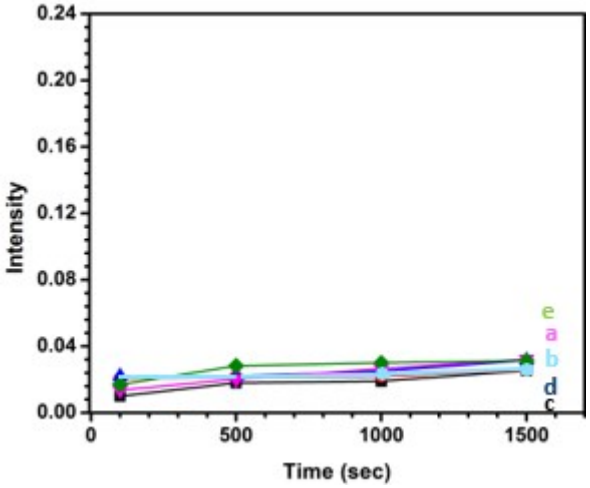

Fig. S7. Plots of peak intensity (peak height) vs time for propane oxidation adsorption at 350 ºC for several major bands detected, including acetate $\upsilon_{as}(CH_3CO_2^-)$ ~ 1560 cm^{-1}(a, pink), acetone $\nu(CH_3)_2C{=}O$) ~1681 cm^{-1}(b,cyan), aliphatic ester υ ($CH_3C(=O)$-O) ~ 1730 cm^{-1} (c, black), bicarbonate υ_{as} ($HOCO_2^-$) ~1644 cm^{-1}(d, blue), formate υ_{as} ($HCOO^-$) ~1593 cm^{-1}(e, green), for $Pd_{31}Au_{69}/Al_2O_3$ (C). The data are extracted from Figure 6.

Table S1 Vibrational mode and position of intermediate species over catalyst surface in range (1200-3000 cm^{-1}). Ref. 17

Species	Vibrational mode	Literature range (cm^{-1})	This work (cm^{-1})
Acetate	V_{as}(COO) V_s(COO)	1550-1590 1458-1470	1560-1580 1455-1460
Acetone	V (C=O) δ (CH)	1668-1725 1434-1436	1681-1683 N/A
Aliphatic ester	V(C=O)	1720-1753	1730-1733
Bicarbonate	V_{as} (OCO) V_s(OCO)	1646-1653 1438-1451	1645
Enolate	V_{as} (CH2=CH-O)	1633-1655	

	V_s (CH2=CH-O)	1392-1419	
	δ (CH)	1335-1338	1373-1376
Formate	V_{as} (COO)	1586-1597	1593
	V_s(OCO)		N/A
	δ (C-H)		N/A
Methoxy	δ_{as} (CH2)	1450-1475	1470, 1455, 1458
Propionate	V_{as} (COO)	1563-1568	
	V_s (COO), δ_{as}(CH3)	1470-1475	N/A
	δ (CH2)		
Water	δ(HOH)	1636-1646	N/A
Carbonate (monodentate)	V_{as} (COO)		1540-1542
	V_s(OCO)		N/A
	V (C-O)		N/A
CO	CO linear gaseous		N/A
CO_2	gaseous		2340-2360
C_3H_8 gaseous	C-H		2968-2070
Hydrocarbon fragments	CH_2(ads) and CH_3 (ads)		2901-2902

Table S2. Summary of values of the apparent rate constant (k_1 and k_2) obtained from fitting curves in Figure 7. The fitting was based on box lucas 2 model; $\theta = (\frac{k_1}{k_1 - k_2})) * (\exp(k_2 * t) - exp(-k_1 * t))$

Catalysts	Surface species	k_1	k_2	k_2/k_1
Pd_9Au_{91}	ester	$8.87x10^{-5}$	$6.07x10^{-4}$	6.84
	acetone	$1.24 x10^{-4}$	$6.69x10^{-4}$	5.39
	bicarbonate	$2.22x10^{-4}$	$9.61x10^{-4}$	4.32
	acetate	$1.29x10^{-4}$	$7.34x10^{-4}$	5.68
	formate	$1.79x10^{-4}$	$7.18x10^{-4}$	4.011
$Pd_{55}Au_{45}$	ester	$1.37x10^{-4}$	$3.77x10^{-4}$	2.75
	acetone	$1.56x10^{-4}$	$5.59x10^{-4}$	3.58
	bicarbonate	$1.76x10^{-4}$	$6.54x10^{-4}$	3.71
	acetate	$2.71x10^{-4}$	$6.87x10^{-4}$	2.53

Table S3. DFT-calculated adsorption energy for molecularly adsorbed propane, O_2, acetate, and C-H on Pd_nAu_{13-n} clusters (n = 1, 6 and 9). Pd (green), Au (yellow), and O_2 (red)

	Pd_{13}	**$Pd_{12}Au_1$**	**Pd_7Au_6**	**Pd_4Au_9**	**Au_{13}**

$CH_3CH_2CH_3$	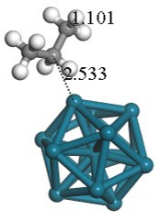	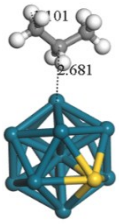	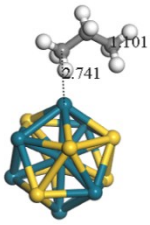	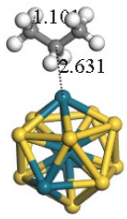	
Ads. energy (eV)	**0.19**	**0.21**	**0.27**	**0.28**	**0.12**
O_2	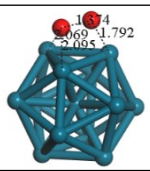	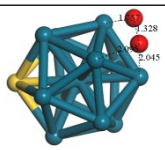	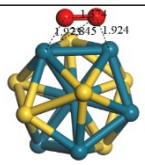	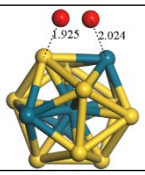	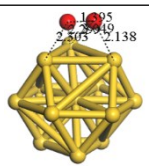
Ads. energy (eV)	**1.53**	**1.46**	**1.19**	**0.82**	**0.41**
CH_3COO	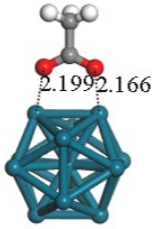	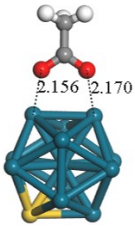	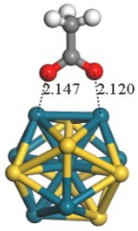	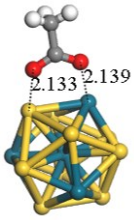	distorted
Ads. energy (eV)	**2.78**	**2.76**	**2.74**	**2.79**	
$CH_3CH_2CH_2$	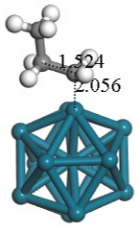	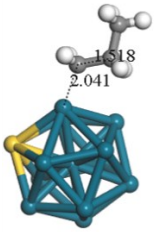	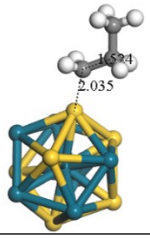	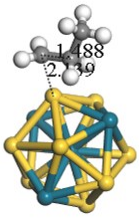	
Ads. energy (eV)	**1.88**	**1.89**	**1.78**	**1.98**	**1.87**
CH_3CHCH_3	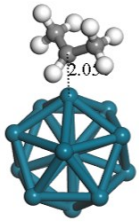	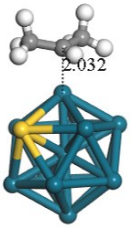	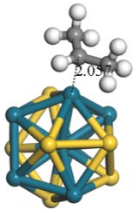		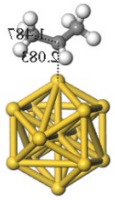
Ads. energy (eV)	**1.76**	**1.78**	**1.7**	**1.72**	**1.7**

Table S4 Structure, binding energy (*E* binding) and Pd-middle carbon distance for Pd_nAu_{13-n} clusters

Composition	Cluster	$E_{binding}$ (eV)	Pd-C distance (Å)
Pd_{13}		2.15	2.64
$Pd_{12}Au_1$		2.15	2.27

Pd_7Au_6		2.13	2.20
Pd_4Au_9		2.05	2.34
Au_{13}		1.87	3.29